A MHZ RATE IMAGING SYSTEM FOR STUDY OF TURBULENT AND TIME EVOLVING HIGH SPEED FLOWS

W. Lempert, B. Thurow, A. Bezant, and M. Samimy
Department of Mechanical Engineering
The Ohio State University
Columbus, OH 43210 USA

ABSTRACT

We present a second generation MHz frame rate imaging system, based on a custom fabricated "pulse-burst" laser and a commercial CCD framing camera. The laser is capable of producing a flexible train of order 30, high intensity pulses, with inter-pulse spacing as short as 1 microsecond. The new system features the incorporation of a Stimulated Brillouin Scattering Phase Conjugate Mirror and has resulted in measured individual pulse energies as high as 180 mJ at the 1.064 micron fundamental wavelength. Second harmonic conversion efficiency as high as 50% has also been obtained.

The utility of the system to capture the dynamics of unsteady and turbulent flow is illustrated by presentation of recent results examining turbulent shear layers produced by Mach 1.3 and 2.0 axisymmetric nozzles. A scheme to measure the convective velocity of large-scale structures is also presented. Application of this approach to measurements of the convective velocity on the Mach 1.3 jet indicate a wide distribution of velocities with an average velocity of 270 m/sec, which is significantly greater than the theoretical value of 206 m/sec. Convective velocity measurements on the Mach 2.0 jet showed the existence of both fast and slow modes, centered around 400 and 200 m/sec, respectively. This is approximately equally spaced around the theoretical value of 303 m/sec. This trend is observed in both the ensemble averaged cross-correlation data as well as the instantaneous histogram data.

Results summarizing the potential feasibility of utilizing the system for extension of the Planar Doppler Velocimetry technique into the “Real Time” regime is also presented. In particular, filtered/unfiltered image pairs were obtained from a Mach 2 rectangular nozzle. While the image quality is severely constrained by speckle noise, the experiments have demonstrated that the real time system has the potential for quantitative determination of velocity fields.

A MHZ RATE IMAGING SYSTEM FOR STUDY OF TURBULENT AND TIME EVOLVING HIGH SPEED FLOWS

W. Lempert, B. Thurow, A. Bezant, and M. Samimy

1. INTRODUCTION

The last decade has seen a literal explosion in the development and application of new laser-based measurement techniques for probing dynamics of fluid flows. The ability to capture time-evolving or volumetric information, however, is severely constrained by limitations of available technology**.** As a general rule, in the gas phase, signal levels for demonstrated imaging diagnostic techniques are sufficiently small that the measurements require high power, nanosecond duration, pulsed sources, such as Q-switched solid-state (principally Nd:YAG) or excimer lasers. The pulse repetition rate of these devices is limited, typically, to the range 10-30 pulses/second for solid-state lasers, and 10-300 pulses/second for excimer lasers. Typical commercially available, high sensitivity digital image sensors, such as CCD cameras, are similarly constrained. This is, in general, too slow, by many orders of magnitude, to track dynamical behavior in high speed - high Reynolds number flow. In this paper, we describe the design and performance of a MHz rate flow imaging system, and demonstrate its utility as a high speed flow diagnostic tool, with a particular emphasis on determination of convective velocity in the shear layers produced by Mach 1.3 and Mach 2.0 axisymmetric free jets**.** Recent progress towards development of "Real Time" Planar Doppler Velocimetry (RTPDV), will also be presented.

2. FACILITIES AND INSTRUMENTATION

Laser System

The laser, illustrated in Fig. 1, is a second generation system based on that described previously by Lempert et al. (1996), Wu, et al (2000) and Thurow et al. (2000,2001). A continuous wave Nd:YAG ring laser serves as the primary oscillator, the output of which is pre-amplified in a double-pass flashlamp-pumped, pulsed amplifier. The resulting, approximately 150 microsecond duration pulse is formed into a "burst" train using a custom, dual Pockel Cell "slicer". The output of the slicer is further amplified in a series of four additional amplifiers and then converted to the second-harmonic wavelength (0.532 microns) with a Type II KTP Second Harmonic Generation (SHG) crystal. The crystal is 8 mm (length) x 12 x 12 (cross section) and is operated at room temperature. The final output is a flexible "burst" of pulses, with inter-pulse spacing as short as 1 microsecond and individual pulse duration as short at 4 nanoseconds. The number and spacing of the pulses is quite flexible, but is ultimately limited by the ~ 100 - 150 microsecond period for which the flashlamp-pumped amplifiers have significant gain. The repetition rate of the burst sequence is as high as 10 Hz, limited by the thermal loading of the amplifiers.

Recently we have incorporated a Phase-Conjugate Mirror (PCM) into the burst mode laser amplifier chain, similar to that which has been employed in pulsed dye lasers (Ni and King, 1996) to remove Amplified Spontaneous Emission (ASE). The PCM consists of a 25.4 mm diameter x 152.4 mm long optical cell, which is filled with a high index-of-refraction liquid, in this case a fluorocarbon known as FC-75. The PCM utilizes the principle of Stimulated Brillouin Scattering (SBS), which is a nonlinear optical phenomenon that produces a coherent beam at 180^{o} ("backscattering") if the pump-beam input achieves a minimum intensity--termed the SBS threshold. As can be seen in Fig 1, the beam is focused into the PCM after the third amplifier (with a 75 mm focal length lens) and is coupled to the final two amplifiers using a quarter wave plate – polarizer combination.

The purpose of the PCM is two-fold. First, we wish to eliminate a low-intensity "pedestal" superimposed upon the high-intensity "pulses" which make up the desired output of the burst train. This pedestal occurs because the Pockel Cell switcher leaks ~ 0.1% when it is nominally "off." Since it is "on" for only ~ 10 nsec out of ~ 10 microseconds, this results in substantial integrated energy in the pedestal. In addition, it appears, although it has not been quantitatively studied, that the pedestal is preferentially amplified, relative to the pulses, in the later stages of amplification. This occurs because in the final two amplifier stages, the intensity gain begins to enter the saturation regime--analogous to attempting to draw too much current out of a typical voltage amplifier. It is believed that the 1000 X weaker pedestal may still be in the "small-signal" (~ 30 X per pass) gain regime when the gain of the higher intensity pulses begin to saturate (to ~ 3-6 in the final two amplifiers). By placing the PCM in the appropriate spot in the amplifier chain, it is possible to exceed the threshold SBS intensity for the desired pulses while keeping the pedestal intensity well below threshold.

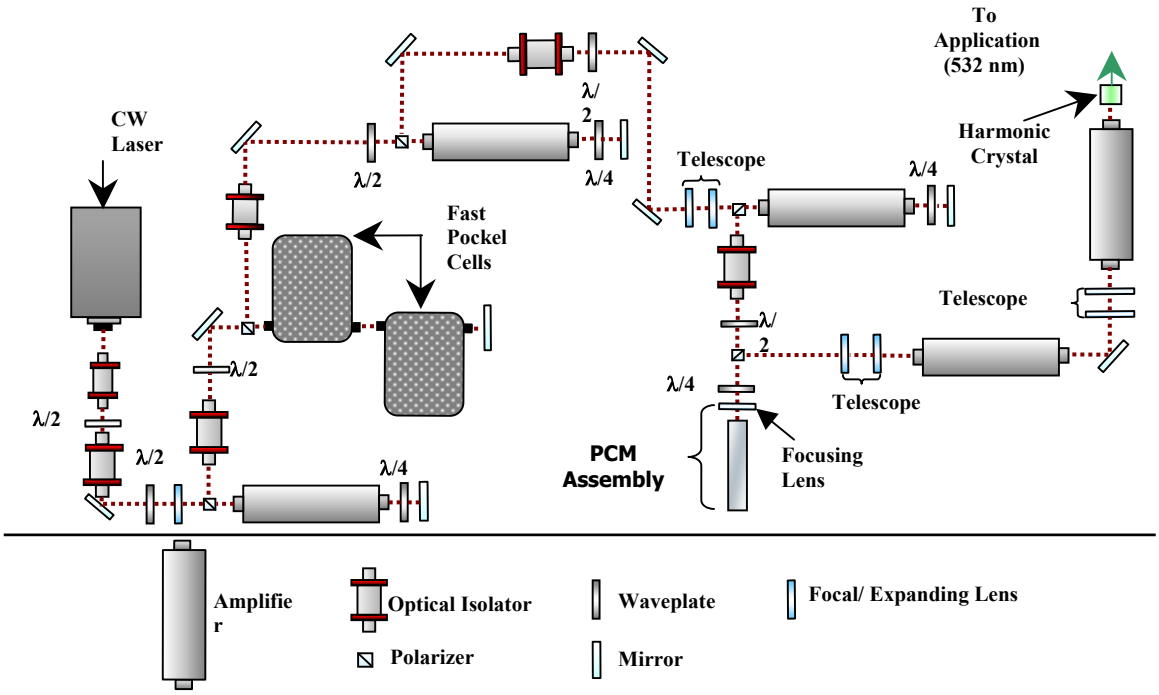

Figure 1: Schematic Diagram of Pulse Burst Laser

The second purpose of the PCM is to provide isolation between the first three stages of amplification and the final two stages. The concern is growth in ASE from the amplifier chain. Similar in some respects to the pedestal problem described above, ASE output is an additional source of temporally broad output energy. Again, by analogy to a voltage amplifier, ASE occurs when the gain is sufficiently high that significant laser system output occurs in the absence of any input from the master oscillator. The second purpose of the PCM is to break the ASE growth chain, which increases exponentially from noise as the laser beam proceeds downstream. Similar to the pedestal described above, the intensity of the ASE component after the third amplifier is well below threshold and, as a result, it passes through the PCM. The build-up process must then start over with the spontaneous emission from the fourth amplifier.

The performance of the burst mode laser has been evaluated for a wide variety of burst sequences and pulse energy levels. In general, it is found that significant energy pulses can be extracted for sequences as long as ~ 120 microseconds, with total energy per burst sequence in the range 1.5 – 1.8 J at the fundamental wavelength of 1.06 microns. Average second-harmonic conversion efficiency as high as 50% was obtained using the 8 mm length Type II KTP crystal. As a typical example, Table I summarizes a recently obtained set of data corresponding to a burst sequence of ten pulses, with inter-pulse spacing of 10 microseconds. In all cases the first four amplifiers were operated at their maximum electrical input energy of 41/41/41/74 J/pulse, respectively. Laser pulse energy at 1.06 microns was obtained as a function of final amplifier-input electrical energy in the range 0 – 110 Joules. However, as a precaution against optical damage to the SHG crystal, harmonic conversion data was only obtained for final amplifier input electrical energy not exceeding 70 Joules. It is stressed that we have been very conservative in the operation of our SHG crystal and that operation in this manner for many weeks has shown no indication of even minor damage to the crystal surface (or to any other optic). We intend, in the near future, to perform a systematic study of optical damage for burst mode operation of sequential, high intensity - nsec duration pulses.

From Table I it can be seen that average energy output as high as 180 mJ per individual pulse has been obtained for this not atypical burst sequence. It can also be seen that SHG conversion efficiency monotonically increases from ~ 24 %, for fundamental pulse energy of 42 mJ/pulse (~ 5 MWatts/cm^2 for our ~ 1cm diameter beam), to 37 % at 120 mJ/pulse (~15 MWatts/cm^2). While not shown in Table I, operation with peak intensity of ~ 30 - 40 MWatt/cm^2 has resulted in a measured SHG conversion efficiency exceeding 50%.

Amp Energy (J)	Average Individual Pulse Energy for Ten Pulse Burst Incorporating Phase Conjugate Mirror (mJ/pulse)		
	1.06 microns	.532 microns	SHG Eff
41/41/41/74/0	42	10	24%
----------/10	44	10.5	24%
----------/20	53	14	26%
----------/30	64	19	30%
----------/40	77	25	32%
----------/50	92	31	34%
----------/60	110	38	35%
----------/70	120	44	37%
----------/80	135	----	----
----------/90	150	----	----
----------/100	165	----	----
----------/110	180	----	----

Table I
Representative 1.06 micron and 0.532 micron energy output for a burst consisting of ten individual pulses with inter-pulse spacing of ten microseconds. All data is averaged over the burst train.

It is also important to determine the uniformity of the individual pulse energy distribution within the overall burst envelope. As would be expected, an inherent trade-off exists between pulse uniformity and pulse energy. As an example, Fig. 2 shows an oscilloscope trace of a typical low-energy 0.532 micron burst train, in this case twenty pulses with an interpulse spacing of 4 microseconds and an average pulse energy (at 0.532 microns) of 2.5 mJ/pulse. While this energy is rather low, it can be seen that the pulse uniformity is exceedingly good.

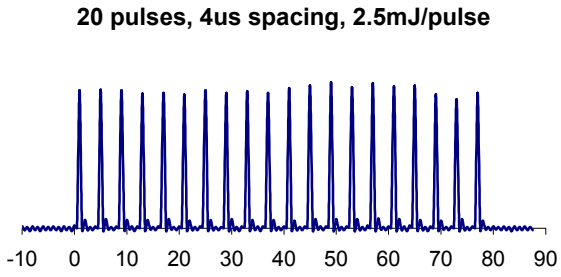

Figure 2: Illustration of Pulse-Energy Uniformity Obtained at Relatively Low Pulse Energy of 2.5 mJ/pulse (at 0.532 microns).

Figure 3 illustrates similar typical oscilloscope traces for higher pulse energies. It can be seen that at these higher energies (30 - 44 mJ/pulse at 0.532 microns), the modulation in the pulse envelope is on the order of +/- 50% of the mean.

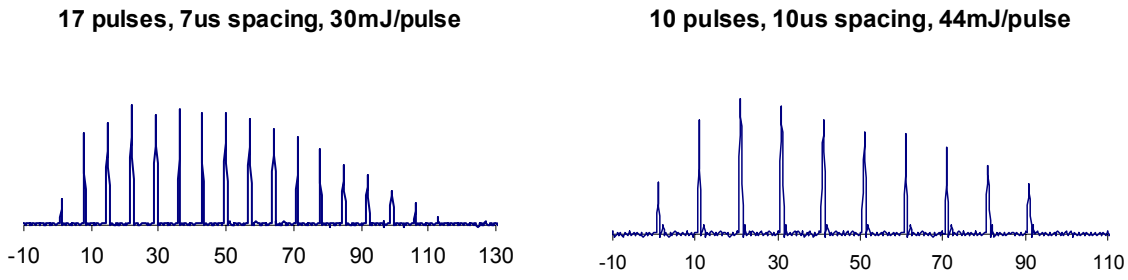

Figure 3: Oscilloscope Traces of Typical Burst Sequences. Trace on right corresponds to PCM data in Table I.

While not specifically examined in this work, previous studies (Lempert, et al., 1997) have determined the spectral characteristics of the burst mode laser to be nearly ideal, with measured spectral linewidth (FWHM) of order 50 MHz for a 16 nsec duration square temporal pulse. While not critical for flow visualization, the linewidth and pulse-to-pulse spectral stability of the laser is critical if it is to be employed for PDV.

Camera System

The camera used in these experiments is manufactured by Silicon Mountain Design (SMD) (now a subsidiary of Dalsa, Inc.). The camera can acquire 17 images at a variable rate as fast as 1 MHz. Each image in the sequence has a resolution of 245 x 245 pixels. The camera is based on a large format (1024 x 1024) 12 bit CCD chip in which sixteen of seventeen pixels are hidden by a custom fabricated mask. The individual pixel aperture size is 9.5 x 9.5 microns with a fill factor of <3%, which, as will be discussed in the final section, significantly impacts Real Time PDV measurements. By appropriate shifting of charge, individual images are initially stored in pixel locations under the mask. After accumulation of all the images, a PC computer reads the output as one large image, containing all 17 frames.

Flow Facility

The flow experiments that will be presented in this paper were conducted at The Ohio State University's Gas Dynamics and Turbulence Laboratory (GDTL). The facility consists of a jet stand and stagnation chamber to which a variety of nozzles may be attached. Air is supplied to the stagnation chamber from two four stage compressors; it is filtered, dried and stored in two cylindrical tanks with a total capacity of 42.5 m^3 at 16.5 MPa (1600 ft^3 at 2500 psi). The stagnation chamber contains a perforated plate and two screens of varying porosity to condition the flow to be as uniform and steady as possible prior to entering the nozzle. The facility has been described in more detail elsewhere (Hileman and Samimy, 2000; Kerechanin, et al., 2001). The two nozzles employed for the flow studies to be presented here have 25.4 mm exit diameters and design Mach numbers of 1.3 and 2.0, the contours of each were designed using the method of characteristics. The actual Mach numbers were measured as 1.28 and 2.06, respectively. The jet exhausts into an anechoic chamber and exits the facility through a large bell-mouth at the opposite end of the chamber. Pressure to the stagnation chamber is controlled manually through the actuation of a Fisher control valve and can be maintained at constant pressure within 0.1 psi. Pressure was set for an ideally expanded flow and held constant through each set of experiments.

3. SUMMARY OF EXPERIMENTS

As an illustrative example of the capabilities of the MHz rate imaging system we present here the results of a recent study of the effects of compressibility on the dynamic behavior of large-scale structures in axisymmetric shear layers. This work has been presented in detail previously (Thurow, et al., 2002), and will, therefore, be only summarized here. To categorize the effect of compressibility, a non-dimensional parameter, the convective Mach number, has been introduced (Bogdonoff, 1989; Papmoschou and Roshko, 1988). For two pressure-matched parallel streams with equal specific heats this parameter is given as:

$$M_c = \frac{U_1 - U_2}{a_1 + a_2} = \frac{U_1 - U_{c,i}}{a_1} = \frac{U_{c,i} - U_2}{a_2} \qquad (1)$$

where U_1 and U_2 are the high- and low-speed free stream velocities, a_1 and a_2 are the speeds of sound and $U_{c,i}$ is the theoretical isentropic convective velocity. Numerous experiments, however, have shown that structures do not convect at the speed indicated in equation 1 (Papamoschou, 1989; Fourgette, et al., 1991; Poggie and Smits, 1996). In particular, experiments performed predominantly on planar shear layers have indicated a significant deviation, which appears as either a 'fast' or a 'slow' mode. This has led to the stream selection rule that states that for a supersonic/subsonic stream combination, the convective velocity will err closer to the high-speed stream while for a supersonic/supersonic combination the velocity will err to the lower speed stream.

In this paper, compressibility effects on axisymmetric jets are studied using real-time "movie" sequences of 17 time-resolved flow visualization images. Spatial cross-correlations are used to track large scale spatial features of the flow with the goal of obtaining a more detailed insight into the effect of compressibility on the convective velocity.

Temporally Resolved Flow Visualization

Figure 4 is a sequence of 4 images taken of the Mach 1.3 (M_c=0.59) jet. Flow is from left to right and the bright regions correspond to areas where moisture in the ambient air has been entrained into the mixing layer and subsequently condensed, creating a "fog" of order 50 nm sized particles. The analysis of the images in Fig. 4 is greatly aided by the addition of 13 other frames that can be played in a movie format, which makes the development and interaction of structures within the mixing layer much easier to visualize. As seen in Fig. 4 (particularly in the upper half of the mixing layer in the 3rd image) one occasionally observes the appearance of structures that resemble the familiar core and braid region associated with incompressible shear layers. These structures do not appear to be globally organized with respect to other structures in the shear layer as they do in incompressible shear layers. Furthermore, the superposition of many smaller scales is evident by the jagged edges at the high- and low-speed boundaries of the mixing layer. Cross-stream image sequences (not shown here) reveal that the structures are quite three-dimensional.

The MHz imaging system provides some additional insights concerning the evolution and mechanisms of interaction between structures. For example, Fig. 4 depicts an event that typifies the dynamics of structures in a compressible mixing layer. In the first frame, three structures are identified and labeled as 'A', 'B' and 'C'. These structures do not appear to be the same as structures seen in incompressible flows, but distinguish themselves from the rest of the mixing layer and are separated by small braid-like regions. In the second frame (which is really the 5th in the full sequence of images), structures 'A' and 'B' are slightly tilted and stretched in the direction of the shear. Structure 'C', meanwhile, appears roughly the same as it did in frame 1, possibly tilting and stretching slightly. In the third frame (9th in the full sequence) structure 'B' is dramatically tilted and stretched from its original shape and now overlaps 'A' on the low-speed side of the mixing layer and 'C' on the high-speed side. In the fourth frame (13th in the full sequence), no evidence of structure 'B' exists as it has been torn apart by the pairing interaction with 'A' and 'C'. Two identifiable structures remain that are labeled 'A+B' and 'B+C' to indicate their origin. The developments characterized in Fig. 4 can be generalized and decomposed into the basic processes of 'tilt', 'stretch', 'tear' and 'pair'. After viewing hundreds of movies, it is quite clear that such processes are very common and take place throughout the mixing layer.

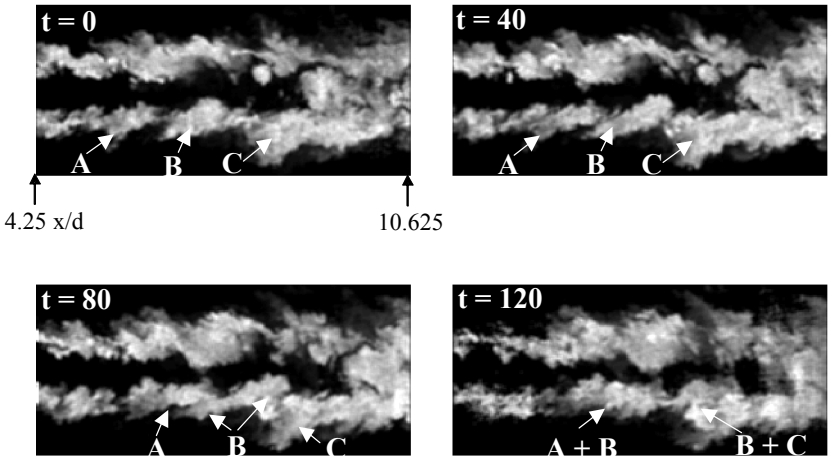

Figure 4 –Temporally resolved flow visualization images of a Mach 1.28 (M_c=0.59) axisymmetric jet

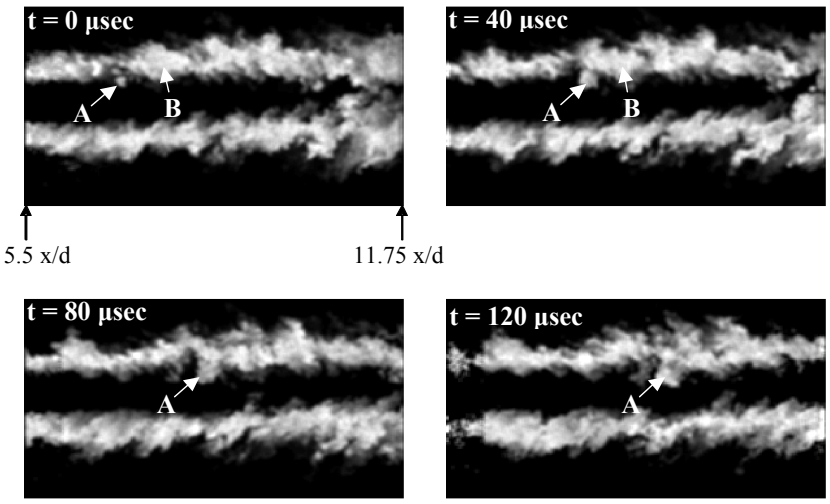

Figure 5 - Temporally resolved flow visualization images of a Mach 2.0 (M_c=0.87) axisymmetric jet.

The Mach 2.0 (Mc=0.87) image sequences exhibit even more three-dimensionality. This is demonstrated by the fluid structure marked 'A' in Fig. 5 which first appears as a small patch of fluid detached from the bulk of the mixing layer. As the flow progresses, this fluid element appears to grow in size, but in reality is convecting into the plane of the laser sheet. This continues to the point such that in the last image it would be difficult to recognize (without the movie sequence) that this fluid element originated from out of the plane. This type of behavior is much more common in the Mach 2.0 jet than it is in the Mach 1.3 jet.

CONVECTIVE VELOCITY MEASUREMENT

Streamwise image sequences such as those demonstrated in Figs 4 and 5 are ideal for determination of convective velocity, which is defined as the velocity with which large-scale structures convect within the flow. From eqn. (1) the predicted values for the Mach 1.3 / 2.0 jets are 206 / 303 m/sec, respectively. As stated previously, however, for convective Mach numbers above 0.5, eqn (1) does not seem to correctly predict the convective velocity.

Recently, we have incorporated a novel algorithm for extraction of convective velocity which takes full advantage of the power of the MHz rate imaging system. The approach has been described in detail previously (Thurow, et al., 2001a) and will, therefore, be only summarized here. The basic idea is to use standard two-dimensional spatial cross-correlation to identify and track a structure as it convects downstream in the mixing layer through the course of the movie. This general approach has been employed by several researchers using image pairs obtained either from two individual lasers or a single double-pulsed laser (for example, Clemens and Mungal, 1995; Elliot, et al., 1995; Smith and Dutton, 1999). The location in the second image where the cross-correlation with the first image is maximum is taken as the displaced location of the structure. The displacement divided by the time delay between the images is defined as the convection velocity. Our approach is similar except, as described in the next section, that information is used from each of the up to 17 images in each movie sequence.

Procedure And Results

All correlations employed a template of dimensions 2δ wide x 1.5δ tall, where δ is the average visual thickness of the mixing layer for a given set of movies. Prior to correlation, individual images are spatially filtered using a 3 x 3 averaging filter. The initial transverse position of the template was chosen to be the center of the mixing layer on the upper side of the layer. The initial streamwise location of the template was set at a fixed position and held constant for each set of images. Varying the streamwise location of the template had minimal effects on the measurements presented here. Note that this procedure is completely automated and does not require any human "selection" of what constitutes a structure. Cross correlation is carried out using a template determined from the first image in the sequence. The location of maximum cross-correlation is then taken as the new location of the structure and the procedure is repeated for subsequent images. Thus the position of a structure can be plotted on an x-t diagram and the slope taken as the convective velocity of the structure. The full sequence of seventeen images

may not be used for each velocity measurement as the structure evolves rapidly and may not be distinguishable in later frames. Knowledge of the structure's position in previous frames, however, is used to limit the cross-correlation calculation only to locations where the structure could physically convect (i.e. not move backwards or faster than jet speed).

Figure 6 is a graph of the ensemble averaged value of the peak correlation for selected time separations in the Mach 1.3 jet. This data was obtained by averaging the two-dimensional spatial cross correlation from an ensemble of ~250 individual movies. The data presented is a one-dimensional slice of the two-dimensional correlations with the slice taken in the streamwise direction through the peak value of correlation. By definition, the maximum correlation for $\Delta t = 0$ μsec is 1.0 and it drops off with increasing streamwise position. For a time separation of 10 microseconds, the correlation level has dropped to about 0.87 and is located about 5 pixels downstream. For increasing time separations, the correlation level drops and the peak broadens. At $\Delta t = 120$ μsec, the maximum correlation is about 0.35 and the peak is quite broad. If one plots the location of this peak on an x-t diagram, the slope of the line fit through the points is the average convective velocity for the Mach 1.3 jet. Such a plot is shown in Fig. 7. The average convective velocity is determined to be 270 m/sec. This velocity is well above the theoretical prediction of 206 m/sec.

Figure 8 is a plot of the ensemble averaged correlation vs. time for the Mach 2.0 jet, obtained from a set of 100 individual movies. A trend similar to that of the Mach 1.3 case is initially observed as the maximum correlation decreases and the peak becomes increasingly broader. For a time separation of 64 microseconds, however, a very interesting event happens. This broad peak can now be distinctly seen as consisting of two peaks. By individually charting the location of both peaks, two convective velocities can be calculated, a 'fast' mode and a 'slow' mode. This is shown in Fig. 9. The local maxima marking the 'fast' mode do not appear until a time separation of 64 μsec. The average velocity of the fast mode is 422 m/sec while that of the slow mode is 185 m/sec. The theoretical value for the convective velocity is calculated as 303 m/sec, which is about halfway between the fast mode and the slow mode. It is worth pointing out that both the fast and slow mode appeared for a variety of window sizes and locations with the average convective velocity not changing by more than 20 m/sec.

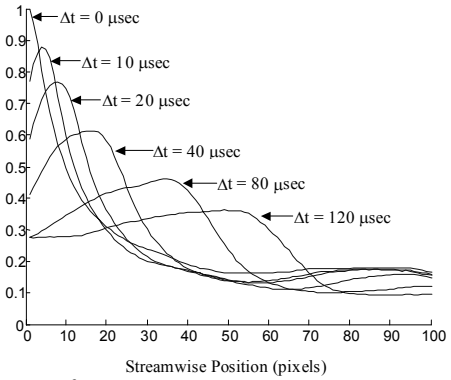

Figure 6 – Streamwise correlation levels for various time separations in a Mach 1.28 axisymmetric jet.

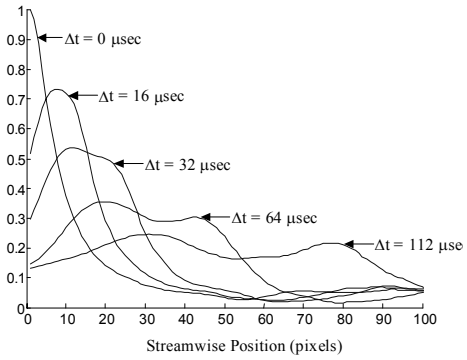

Figure 8 – Streamwise correlation levels for various time separations in a Mach 2.06 axisymmetric jet.

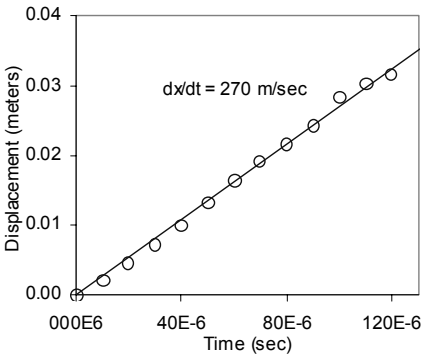

Figure 7 – Plot of peak location vs time for Mach 1.28 axisymmetric jet.

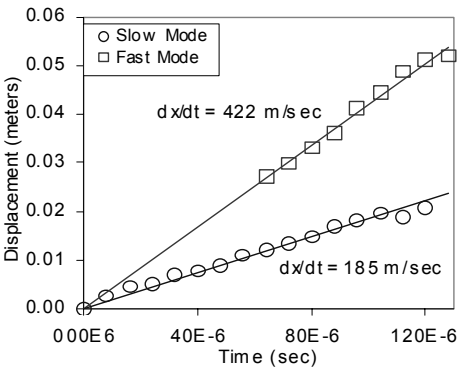

Figure 9 – Plot of peak locations vs. time for Mach 2.06 axisymmetric jet.

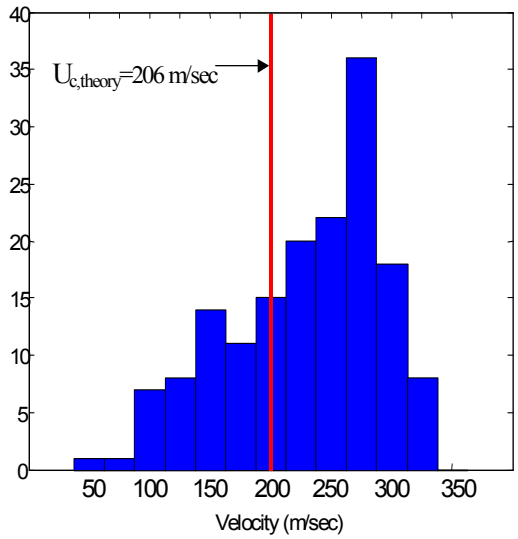

Figure 10 – Histogram of convective velocities for Mach 1.3 jet.

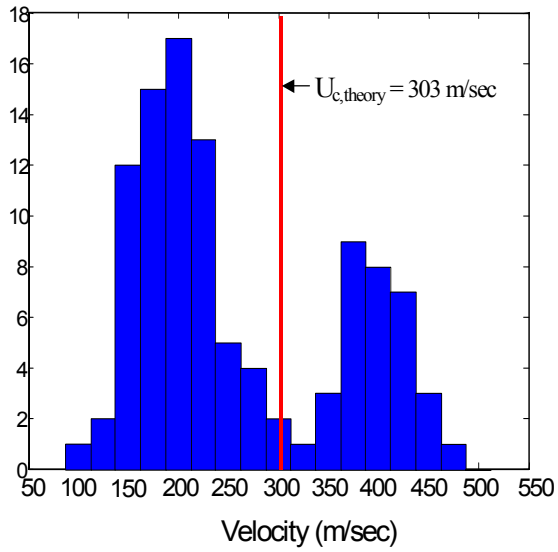

Figure 11 – Histogram of convective velocities for Mach 2.0 jet.

Additional details can be obtained from examination of the cross-correlation data for individual image sets, which provides a histogram of "instantaneous" convective velocities. Figure 10 is a histogram of the convective velocity for the Mach 1.3 jet. This data includes structures from both the upper and lower halves of the mixing layer. The peak of the histogram is centered around 275 m/sec, which is close to the ensemble average velocity measurement obtained earlier. The broad peaks in the cross-correlations in Fig. 6 are likely due to this distribution.

Figure 11 is a histogram of the convective velocities for the Mach 2.0 jet. It consists of 104 individual measurements. Clearly, the fast and slow modes observed in the ensemble average data are manifested in the bimodal peaks. These peaks are centered at about 200 and 400 m/sec and are close to the ensemble average values given earlier. Each distribution is nearly Gaussian in shape and appear to be evenly displaced from the theoretical value of 303 m/sec. Roughly 2/3 of the measurements are of the slow mode. The change in shape of the histogram was examined for various window sizes. The main features of Figure 11 were largely insensitive to any change in window size. For smaller window sizes, the overall distribution was not as smooth, but distinct peaks still occurred around 200 and 400 m/sec.

The convective velocity results presented here are, to our knowledge, unique and worthy of some additional discussion. The deviation of the convective velocity from the theoretical isentropic value is not a surprise and has led to the formulation of the stream selection rule. What is new and surprising about these results, however, is the presence of fast and slow modes in the Mach 2.0 jet. To our knowledge, all previous convective velocity data studies in compressible shear layers have indicated the presence of only a single mode. Possible explanations for this behavior are described in more detail in Thurow, et al., (2002).

It is worth noting, however, that the presence of fast and slow modes has been observed in three-dimensional linear stability analyses of compressible shear layers. These studies by Jackson and Grosch (1989) and Day, et al. (1998) show that for convective Mach numbers greater than 1.0, outer modes of instability waves (fast and slow modes) develop that become more amplified with increasing compressibility. These modes are in addition to the central mode, which dominates at convective Mach numbers below 1.0. Furthermore, the amplification rate of the outer modes does not become significant until convective Mach numbers much greater than the 0.87 in this study. Clearly, however, there is the possibility that these modes are related to observed convective velocities seen here.

4. REAL TIME PDV

Finally, we briefly summarize recent progress towards our ultimate goal of developing quantitative Real Time PDV (Thurow, et al., 2001b). PDV utilizes the frequency shift of laser light after it is scattered by moving particles. Similar to planar imaging velocimetry (PIV), the technique yields an instantaneous snapshot of the velocity field. More specifically, when a narrow spectral linewidth laser is incident to a flow field, scattering (by particles or molecules) is spectrally shifted due to the Doppler effect. If a cell filled with a suitable atomic or molecular vapor is placed in front of the detector, then the fractional transmission through the cell constitutes a unique determination of

the component of velocity parallel to the wave-vector. (This direction is perpendicular to the vector, which bisects the angle between the laser and the detector). If a laser beam is formed into a thin sheet, and if the filtered scattering is detected with a CCD imaging device, then instantaneous planar velocity images can be obtained. To achieve this, a pair of matched field-of-view images, one filtered and one unfiltered, are obtained and velocity field determined by pixel by pixel ratioing. PDV has developed to the point where reliable velocity measurements with errors on the order of 2 m/sec are readily obtainable for a variety of flow environments. More detail can be found in recent comprehensive review articles by McKenzie (1996), Elliott and Beutner (1999), and Samimy and Wernet (2000).

As a preliminary test of the feasibility of Real Time PDV, images were obtained from an acetone seeded, high aspect ratio Mach 2 rectangular half nozzle with dimensions 1/8" x 3/4". We note that this work was performed prior to addition of the PCM and fifth amplifier to the burst mode laser so that the individual pulse energy at 0.532 microns was limited to ~ 2 mJ. The sheet propagated downward to the vertical jet, incident at an angle of ~ 15 degrees with respect to the streamwise direction, thus forming a quasi-streamwise view. Scattering was captured at 90^{o} to the jet, with a field of view of approximately 1.6" x 0.8".

A sample raw image pair is shown in Fig. 12. (The image is slanted due to the method in which the camera acquires and reads out the image). The left-hand side of the frame contains the unfiltered image while the right-hand side contains the filtered image. This figure demonstrates the ability of the system to capture both images on a single camera, but also illustrates constraints due to the limited power available from the earlier version of the laser. Note that the image is scaled from 0 to 140 intensity units out of a maximum of 4095. The spatial resolution of the camera appears to be sufficient to make measurements on a variety of scales within the flow.

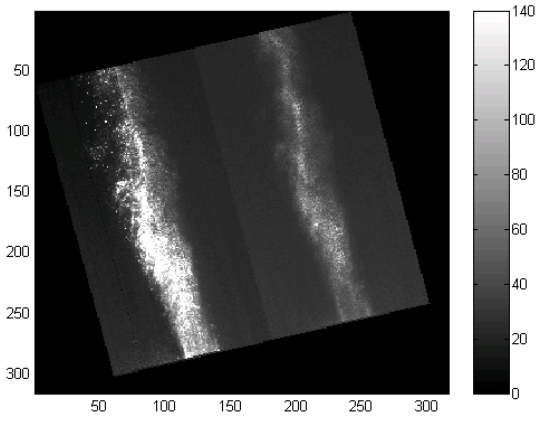

Figure 12: Sample unfiltered (left) and filtered (right) image pair obtained with RT-PDV.

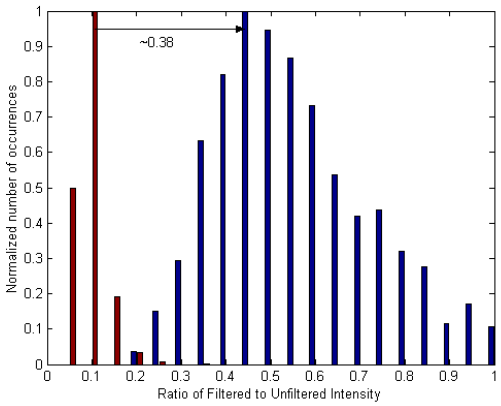

Figure 13: Histogram of transmission ratios for Mach 2.0 nozzle (right) and stationary target (left) obtained from image pairs such as that of Fig. 12. Corresponding bulk Doppler shift is 732 MHz.

Figure 13 shows a histogram of intensity ratios obtained from image pairs similar to that shown in Fig. 12. This histogram also plots a reference point taken immediately afterwards on a stationary target. Two things are clear from this figure. First, the velocity of the Mach 2 flow is clearly resulting in a bulk Doppler shift of ~0.38 dimensionless "ratio" units. This shift corresponds to a mean frequency shift of 732 MHz, which translates into an average streamwise velocity on the order of 400 m/sec. Second, the histogram of values obtained with the jet on is much broader than the histogram obtained with no flow. The large spread is an indication of the range of velocities being measured in the flow.

These promising, albeit preliminary, results indicate that the PDV apparatus incorporating the pulse burst laser and ultra-fast camera is detecting and measuring Doppler shifted scattering. Currently, however, the signal to noise ratio in the images is quite low (of order 5), dominated by large contributions of noise, thought to be the result of what is known as 'speckle'. Speckle is a well known phenomenon, which accompanies scattering of coherent radiation, caused, fundamentally, by spatial interference that leads to random intensity minima and maxima in the image. It is well established that speckle is the dominant noise source in PDV (Smith, 1998) and is minimized by incorporating large camera pixels and collection lens solid angles. As discussed in more detail in Thurow, et al (2001b), the relatively small pixel size (~9 micron aperture) of the framing camera employed for this study is

thought to be a significant issue which needs to be addressed. We have recently obtained a new larger pixel format, framing camera, which shows great promise for mitigation of speckle noise as well as increased signal. In combination with the approximate factor of ten increase in currently available pulse energy it is anticipated that much higher quality PDV "movies" will be obtained in the near future.

5. CONCLUSIONS

A second generation MHz rate imaging system has been developed, which combines a home built Nd:YAG burst mode laser and a commercial framing CCD camera. The laser is capable of producing a flexible train of order 30, high intensity pulses, with inter-pulse spacing as short as 1 microsecond. The system features the incorporation of a Phase Conjugate Mirror which acts as an intensity dependent mirror, and serves the purpose to remove an unwanted low intensity, quasi-continuous pedestal which sits underneath the desired pulse train, and to remove amplified spontaneous emission, which limits the achievable gain. Individual pulse energies as high as 180 mJ at the 1.06 micron fundamental wavelength have been obtained from the current system, with second harmonic conversion efficiency as high as 50%.

The system has been employed to examine turbulent shear layers produced by Mach 1.3 and 2.0 axisymmetric nozzles. A scheme to measure the convective velocity of large scale structures was also developed, which tracks the structures through the sequence of images. Application of this approach to measurements of the convective velocity on the Mach 1.3 jet indicate a wide distribution of velocities with an average velocity of 270 m/sec, which is significantly greater than theoretical velocity of 206 m/sec. Convective velocity measurements on the Mach 2.0 jet showed the existence of both fast and slow modes centered around 400 and 200 m/sec respectively. This is equally spaced from the theoretical velocity of 303 m/sec. This trend is observed in both the ensemble averaged cross-correlation data as well as the instantaneous histogram data.

The potential feasibility of incorporating the MHz rate imaging system for extension of the Planar Doppler Velocimetry technique into the "Real Time" regime has been explored with a series of preliminary measurements. In particular, filtered/unfiltered image pairs were obtained from a Mach 2 rectangular nozzle. While the image quality is severely constrained by speckle noise and low signal level, the experiments have demonstrated that the real time system has the potential for quantitative determination of velocity field. It is anticipated that incorporation of a camera with larger pixel format and the PCM in the pulse burst laser will result in significant improvement in velocity measurement accuracy.

6. ACKNOWLEDGEMENTS

The authors acknowledge the assistance of Mr. Mark Stevens, who assembled the phase conjugate mirror as a portion of his undergraduate honors thesis, and Mr. James Hileman, who assisted in many of the flow measurements. The authors also acknowledge the support of Innovative Scientific Solutions, Inc., through a sub-contract from NASA Glenn Research Center, and from the National Science Foundation and the State of Ohio Hayes Investment Fund. Brian Thurow would also like to thank the Department of Defense for a National Defense Science and Engineering Graduate fellowship.

REFERENCES

Bogdanoff, D. W., "Compressibility Effects in Turbulent Shear Layers," *AIAA. J.* , Vol. 21, 926, 1983.

Clemens, N.T. and G.M. Mungal, (1995), "Large-scale Structure and Entrainment in the Supersonic Mixing Layer," *Journal of Fluid Mechanics,* Vol. 284, pp. 171-216.

Day, M. J., Reynolds, W. C. and Mansour, N. N., (1998), "The Structure of the Compressible Reacting Mixing Layer: Insights from Linear Stability Analysis," *Phys. of Fluids*, Vol. 10, pp. 993-1007, 1998.

Elliott, G.S., M. Samimy, and S.A. Arnette, (1995), "The Characteristics and Evolution of Large Scale Structures in Compressible Mixing Layers," Physics of Fluids, Vol. 7, pp. 864-876.

Elliott, G. and T. Beutner, (1999), "Molecular Filter Based Planar Doppler Velocimetry," *Progress in Aerospace Sciences*, Vol. 35, pp. 799-845.

Fourgette, D. C., Mungal, M. G., and Dibble, R. W., (1991), "Time Evolution of the Shear Layer of a Supersonic Axisymmetric Jet," *AIAA Journal*, Vol. 29, No. 7, pp. 1123-1130.

Hileman, J. and M. Samimy, (2000), "An Attempt to Identify Noise Generating Turbulent Structures in a High Speed Axisymmetric Jet," AIAA Paper 2000-2020, June 2000.

Jackson, T. L. and Grosch, C. E., (1989), "Inviscid Spatial Stability of a Compressible Mixing Layer," *J. Fluid Mech.*, Vol. 28, pp. 609-622.

Kerechanin, C.W. , M. Samimy, and J-H Kim, (2001), "Effects of Nozzle Trailing Edge Modifications on Noise Radiation in a Supersonic Rectangular Jet,"AIAA Journal, Vol. 39, No. 6, pp. 1065-1070, 2001.

Lempert, W.R., P-F Wu, B. Zhang, R.B. Miles, J.L. Lowrance, V. Mastracola, and W.F. Kosonocky, (1996), "Pulse-Burst Laser System for High Speed Flow Diagnostics", Paper #AIAA 96-0500, AIAA 34th Aerospace Sciences Meeting, Reno, NV, Jan. 15-18, 1996.

Lempert, W.R., P.-F. Wu, and R. B. Miles, (1997), "Filtered Rayleigh Scattering Measurements Using a Pulse-Burst Laser System," Paper #AIAA 97-0500, AIAA 35th Aerospace Sciences Meeting, Reno, NV, Jan. 6-9, 1997.

McKenzie, R.L.(1996), "Measurement Capabilities of Planar Doppler Velocimetry Using Pulsed Lasers," *Applied Optics*, Vol. 35, No. 6, pp. 948-964.

Ni, C.K. and Kung, A.H, (1996), "Effective suppression of amplified spontaneous emission by stimulated Brillouin scattering phase conjugation", Optics Letters, Vol. 21, pp. 1673-1675.

Papamoschou, D., and Roshko, A., (1998), "The Compressible Turbulent Shear Layer: An Experimental Study," *Journal of Fluid Mechanics*, Vol. 197, pp. 453-477.

Papamoschou, D., (1989). "Structure of Compressible Turbulent Shear Layer," AIAA Paper 89-0216.

Poggie, J. and Smits, A. J., (1996), "Large-Scale Coherent Turbulence Structures in a Compressible Mixing Layer Flow," AIAA Paper 96-0436.

Samimy, M. and M.P. Wernet, (2000), "Review of Planar Multiple-Component Velocimetry in High-Speed Flows," *AIAA J.*, Vol. 38, No. 4, pp. 553-574.

Smith, M.W. (1998), "The Reduction of Laser Speckle Noise in Planar Doppler Velocimetry Systems," AIAA Paper 98-2607, June 1998.

Smith, K.M. and J.C. Dutton, (1999), "Evolution and Convection of Large-scale Structures in Supersonic Reattaching Shear Flows," *Physics of Fluids,* Vol. 11, No. 8, pp. 2127-2138.

Thurow, B., W. Lempert, and M. Samimy, (2000), Paper AIAA-2000-0659, 38th AIAA Aerospace Sciences Meeting, Reno, NV. Jan 10 - 13, 2000.

Thurow, B., J. Hileman, M. Samimy, and W. Lempert, (2001a), "An In-Depth Investigation of Large Scale Structures in a Mach 1.3 Axisymmetric Jet," Paper AIAA-2001-0148, 39th AIAA Aerospace Sciences Meeting, Reno, NV, Jan. 8 - 11, 2001.

Thurow, B., J. Hileman, M. Samimy, and W.R. Lempert, (2001b), "Progress Towards a Real-Time Quantitative Measurement Technique for High Speed Flows, AIAA Paper 2001-2985, 31st AIAA Fluid Dynamics Conference, Anaheim, CA, June 11-14, 2001.

Thurow, B., J. Hileman, M. Samimy, and W. R. Lempert, (2002), "Compressibility Effects on the Growth and Development of Large-Scale Structures in an Axisymmetric Jet, Paper AIAA-2002-1062, 40th AIAA Aerospace Sciences Meeting, Reno, NV, January 14-17,2002.

Wu, P., W. R. Lempert, and R.B. Miles, (2000), "MHz Pulse-Burst Laser System and Visualization of Shock-Wave/Boundary-Layer Interaction in a Mach 2.5 Wind Tunnel," AIAA Journal 38, pp. 672-679.